Biosensors and Bioelectronics 68 (2015) 122–128

Contents lists available at ScienceDirect

Biosensors and Bioelectronics

journal homepage: www.elsevier.com/locate/bios

Attomolar quantitation of *Mycobacterium tuberculosis* by asymmetric helicase-dependent isothermal DNA-amplification and electrochemical detection

Susana Barreda-García [a], María José González-Álvarez [a], Noemí de-los-Santos-Álvarez [a], Juan José Palacios-Gutiérrez [b], Arturo J. Miranda-Ordieres [a], María Jesús Lobo-Castañón [a,*]

[a] Dpto. Química Física y Analítica, Universidad de Oviedo, Julián Clavería 8, 33006 Oviedo, Spain
[b] Servicio de Microbiología, Unidad de Referencia Regional de Micobacterias de Asturias. Hospital Universitario Central de Asturias, Avda Roma s/n, 33011 Oviedo, Spain

ARTICLE INFO

Article history:
Received 25 September 2014
Received in revised form
2 December 2014
Accepted 11 December 2014
Available online 12 December 2014

Keywords:
Isothermal amplification
Helicase
Mycobacterium tuberculosis
Electrochemical biosensor
Hybridization assay

ABSTRACT

A highly sensitive and robust method for the quantification of specific DNA sequences based on coupling asymmetric helicase-dependent DNA amplification to electrochemical detection is described. This method relies on the entrapment of the amplified ssDNA sequences on magnetic beads followed by a post-amplification hybridization assay to provide an added degree of specificity. As a proof-of-concept a 84-bases long sequence specific of *Mycobacterium tuberculosis* is amplified at 65 °C, providing 3×10^6 amplification after 90 min. Using this system 0.5 aM, corresponding to 15 copies of the target gene in 50 μL of sample, can be successfully detected and reliably quantified under isothermal conditions in less than 4 h. The assay has been applied to the detection of *M. tuberculosis* in sputum, pleural fluid and urine samples. Besides this application, the proposed assays is a powerful and general tool for molecular diagnostic that can be applied to the detection of other specific DNA sequences, taking full advantage of the plethora of genomic information now available.

1. Introduction

The huge amount of genomic data now available is posing new problems and challenges to analytical chemistry. To harvest all this information, there is a real need to explore new sensitive and reliable methods for the quantification of specific nucleic acid sequences in such diverse fields as food safety, environmental monitoring, and clinical diagnosing. These methods should also be easy-to-use and cost-effective so that access to molecular assays can be available to poorly equipped laboratories or even for point of care control (Niemz et al., 2011).

General hybridization assays and genosensors prove to be especially powerful in the rapid and sensitive detection of synthetic short oligonucleotides (Sassolas et al., 2008). But when faced with genomic DNA, the complexity of the target and sample media limits their application. Even in the cases where the hybridization assays show analytical sensitivity high enough to detect the very low amounts of DNA required (Nam et al., 2004), a sample pretreatment to restrict the size of the target and facilitate hybridization is usually necessary (Hill et al., 2007; Minunni et al., 2005). Although in some cases a simple DNA fragmentation has proven sufficient (Corrigan et al., 2013), most of the strategies developed to date rely on coupling the hybridization assays to target amplification methods, contributing to both specifically amplify the target and restrict its size. Polymerase chain reaction (PCR) is the gold standard (Lucarelli et al., 2005; Pedrero et al., 2011), but most genosensors have been validated using serial dilutions of a single PCR-amplified sample. This strategy prevents the establishment of the relationship between the readout and the amount of copies of genomic DNA, without taking into account the kinetics and efficiency of the coupled PCR process. Additionally, PCR amplicons are usually longer than ideal for coupling to surface-hybridization process, which often results in a decrease in the sensitivity and/or an increase in the assay time when compared with short oligonucleotides sequences (Miranda-Castro et al., 2009; Martín-Fernández et al., 2014). From an instrumental point of view, the need for thermal cycling and accurate temperature control also limits the use of PCR to centralized laboratories.

To overcome these drawbacks different isothermal amplification methods have been developed (Craw and Balachandran, 2012; Li and Macdonald, 2015) employing various strategies to achieve strand separation at a constant temperature as opposed to thermal

* Corresponding author.
E-mail address: mjlc@uniovi.es (M.J. Lobo-Castañón).

http://dx.doi.org/10.1016/j.bios.2014.12.029
0956-5663/

strand separation in PCR. These involve either the use of strand displacement polymerases combined with especially designed primers or probes, as is the case in loop-mediated amplification (LAMP) (Hataoka et al., 2004; Hsieh et al., 2012; Notomi et al., 2000), and rolling-circle amplification (RCA) (Tanaka et al., 2011; Zhao et al., 2008), or mimicking in vivo DNA replication utilizing different enzymes such as endonucleases (Connolly and Trau, 2010; Shi et al., 2014; Tan et al., 2005), recombinases (Shen et al., 2011) or helicases to promote denaturation. Among them, helicase dependent amplification (HDA) is one of the simplest approaches that closely resembles PCR reaction scheme but at a constant temperature, in the presence of helicase for DNA unwinding. Since its first description (Vincent et al., 2004), it has been applied to the detection of several pathogen organisms mainly using electrophoresis (Barbieri et al., 2014), colorimetric (Ao et al., 2012) or fluorimetric (Tong et al., 2012) detection of amplicons. It has also been carried out directly on the surface of microarrays (Andresen et al., 2009) or integrated with microfluidic (Mahalanabis et al., 2010; Ramalingam et al., 2009) and vertical flow strip systems (Jordan et al., 2012) for developing portable devices that can be used in point-of-care testing. However, despite the great potential of electrochemical detection to obtain a simple and compact system, there are only two reported strategies coupling HDA with this kind of detection (Kivlehan et al., 2011; Torres-Chavolla and Alocilja, 2011) both with a symmetric amplification format. These studies did not test the assay in genomic DNA and displayed limited detectability, remarkably when the detection is performed using a heterogeneous hybridization assay for which a limit of detection as high as 3 nM (0.1 ng/μL for a 105 bp target) is reported (Torres-Chavolla and Alocilja, 2011), presumably due to interference from non-specific amplification products.

This is certainly one of the main limitations of HDA reaction; owing to the use of low temperatures for amplification the problems associated to primer dimers and mis-priming increase. This can sometimes lead to long non-specific byproducts that can be confused with target products (Mahalanabis et al., 2011), especially when a DNA intercalating probe is used for detection.

In this study, a novel DNA quantification system has been developed combining asymmetric HDA amplification, post-amplification hybridization and electrochemical enzyme-mediated detection. Our system leverages the asymmetric primer ratio to limit the amount of non-specific products generated. In addition, the relatively short single-stranded amplicons (80–120 bp) obtained in HDA are trapped onto magnetic microparticles and detected by hybridization to a fluorescein-tagged probe, improving assay selectivity. We demonstrate that the system can be used to quantitatively detect a model *Mycobacterium tuberculosis* (MTB) gene down to 0.5 aM, three orders of magnitude below the limit of detection of a real-time fluorescence HDA system. As a demonstration of our system capability, we report the quantitative detection of MTB in sputum, urine, and pleural liquid clinical specimens.

2. Experimental section

2.1. HDA amplification

The HDA primers that we employed are designed to amplify an 84 bp DNA fragment from the insertion sequence IS6110 (GenBank accession no. X17348) (Motré et al., 2011). This gen is present in the MTB complex in multiple copies and is specific for tuberculosis causing bacteria. Within this sequence, the forward (52% GC) and reverse (54% GC) primers span bases 962–986 and 1020–1045, respectively; the antisense primer is labeled with biotin at the 5´-terminal.

DNA templates comprising either synthetic oligonucleotides or genomic DNA from clinical isolates were amplified using the

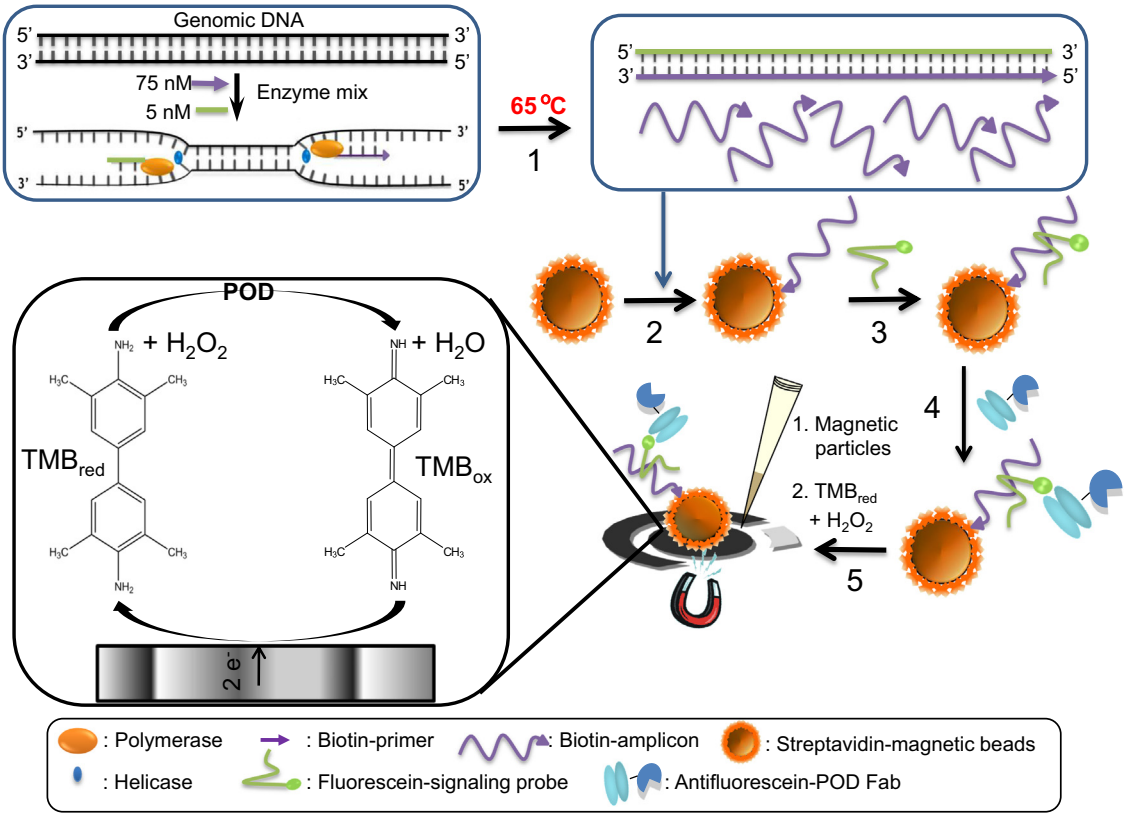

Scheme 1. Overview of the different steps of the aHDA-electrochemical-genomagnetic assay.

IsoAmp® II kit (BioHelix, Beverly, USA) (step 1, Scheme 1). The reactions were carried out in an oven at 65 °C using a 2-step protocol, following the operations described in Supporting information.

The product of the symmetric amplification was analyzed by agarose gel electrophoresis, using a 2% agarose gel stained with ethidium bromide and visualized through an UV transilluminator.

For real-time monitoring of the amplicons the reactions were performed in the presence of Evagreen and ROX in a HT7900 real-time thermocycler (Applied Biosystems®) set to 66 °C for 5 s and 65 °C for 115 s. Fluorescence of the mixture was monitored over a period of 1 h.

2.2. Quantitative analysis of amplicons

The biotinylated strands in the amplicons were entrapped through biotin–streptavidin interaction onto magnetic microparticles (step 2, Scheme 1). 50 μL of the amplified mixture, without any purification, were diluted to 500 μL with a 5 mM Tris–HCl, 1 M NaCl solution and transferred to a tube containing 50 μg of the streptavidin-modified magnetic particles previously washed with the same solution containing 0.005% Tween 20. After a 15 min incubation at room temperature the beads were magnetically separated and washed twice with 500 μL of 5 mM Tris–HCl, 0.1 M NaCl buffer containing 0.005% Tween 20. Then, they were re-suspended in 500 μL of 5 mM Tris–HCl, 0.1 M NaCl containing 75 nM of a 20-mer fluorescein-tagged probe complementary to an internal sequence of the amplified fragment, and incubated for 30 min at room temperature (step 3, Scheme 1). After two new washing steps in casein blocking buffer (0.5% in PBS 1 ×), we performed the enzymatic labeling by re-suspending the microparticles in 500 μL of the blocking solution containing 0.5 U/mL of anti-fluorescein–POD conjugate (step 4, Scheme 1). After 10 min of incubation time, the beads were washed twice with 1 × PBS and re-suspended in 500 μL of the same buffer. 15 μL of the fully-modified beads were finally magnetically captured onto the working electrode of a screen printed cell (step 5, Scheme 1) by means of a magnet placed under it. The cell was covered with 25 μL of tetramethylbenzidine (TMB)+H_2O_2 solution followed by chronoamperometric measurement of the oxidized product after 30 s of enzymatic reaction using a potential pulse to 0 V, and sampling the current during 60 s.

Initial calibration tests were performed with synthetic oligonucleotides equivalent to the HDA products, and obtained via commercial synthesis (Table S1), both as ssDNA and dsDNA. When dsDNA is measured, the desired amount of target DNA and 75 nM signaling probe in 5 mM Tris–HCl, 0.1 M NaCl were incubated at 98 °C for 5 min, followed by cooling in an ice bath for another 5 min before trapping the duplex onto the magnetic beads.

2.3. Preparation of clinical samples

Clinical specimens were processed according to standard accepted methods. All samples, except the pleural fluid were decontaminated by the N-acetyl-L-cysteine–sodium hydroxide (NALC–NaOH) method, and concentrated by centrifugation. This step was performed using the commercial kit MycoPrep™ (Becton-Dickinson). Briefly, samples were mixed with an equal volume of NALC–NaOH solution containing 0.5 M NaOH, 0.37 g/L N-acetyl-L-cysteine and 0.05 M trisodium citrate dihydrate. After incubation for 15 min at room temperature, samples were neutralized by adding phosphate buffer and subjected to centrifugation (20 min, 3000*g*). The sediment was resuspended in phosphate buffer pH 6.8 (2 mL). A small amount of the suspension was used to prepare smears for Ziehl–Neelsen staining (acid fast staining), and after microscopic observation semi-quantitative results were expressed as number of acid-fast bacilli (AFB) per field according to Centers for Disease Control/American Thoracic Society (CDC/ATS) and World Health Organization (WHO) guidelines. 1.5 mL of the same resuspended samples was employed for the culture media (both the mycobacteria growth indicator tube (MGIT) and the classical Löwenstein–Jensen media) and real time PCR analysis, RTi-PCR (Xpert® MTB/RIF, Cepheid, USA). RTi-PCR was performed according to manufacturer instructions. The remaining DNA extracts, obtained in a sonication mechanical procedure, were stocked at −80 °C and used for aHDA amplification coupled to the genomagnetic assay.

3. Results and discussion

We have devised a simple way of coupling isothermal DNA amplification to electrochemical detection of the amplified products that is illustrated in Scheme 1. Asymmetric HDA (aHDA) reaction of MTB-specific sequences, using a biotin-tagged reverse primer in excess to the direct primer, boosts the generation, at a constant temperature, of biotinylated single-stranded amplicons copy of the initial genomic DNA used as target (Scheme 1, step 1). These amplicons are trapped onto the surface of streptavidin-modified magnetic beads through affinity interaction (Scheme 1, step 2). The third step is the hybridization-based detection of amplicons employing a fluorescein-tagged signaling probe, complementary to an internal sequence within the amplicon. Upon hybridization, a monovalent enzymatic label is held on the magnetic particle surface by incubation with anti-FITC–POD conjugate, Fab fragment (Scheme 1, step 4). The bound enzyme activity is then chronoamperometrically quantified by entrapping the magnetic beads onto screen-printed carbon electrodes with the aid of a magnet (Scheme 1, step 5). The amount of the oxidized substrate enzymatically produced is directly related to the amount of copies of genomic DNA in the original sample. Optimal design for efficient amplification reaction and sensitive hybridization-based electrochemical detection is described below.

3.1. Evaluation of HDA amplification

We started qualitatively exploring HDA amplification. To this end, 0.1 nM synthetic target, genomic DNA extracted from a MTB clinical isolated, and a negative control (background amplification) were subjected to amplification at 65 °C for 90 min in the presence of both primers, 200 nM each. Analysis of the amplification products by agarose gel electrophoresis revealed a single strong band from both synthetic and clinical samples, corresponding to products of the expected size (Fig. S1). In the absence of target DNA a faint band corresponding to smaller products was also observed. After amplicon isolation, the generated amplicons were cloned and sequenced to verify their identity. All the clones from the samples showed an 84-bases long sequence identical to the selected target, confirming the selectivity of the amplification. In contrast, from the negative control a side product 52 bases long, corresponding to the direct primer and the sequence complementary to the reverse one, just separated by a single base (cytosine), was obtained. The mechanism of formation of this product is not fully understood but it cannot be distinguished from the specific product when using intercalating agents for detection.

The kinetic of the amplification was monitored in real time by using EvaGreen, a double-stranded DNA binding dye that shows fluorescence enhancement after binding. Amplification of different copies of target DNA from 1 fM to 1 pM in the presence of two different primer concentrations, within the range recommended for HDA, 75 nM and 200 nM, was examined. In both cases sigmoid curves similar to that obtained in standard real-time PCR were

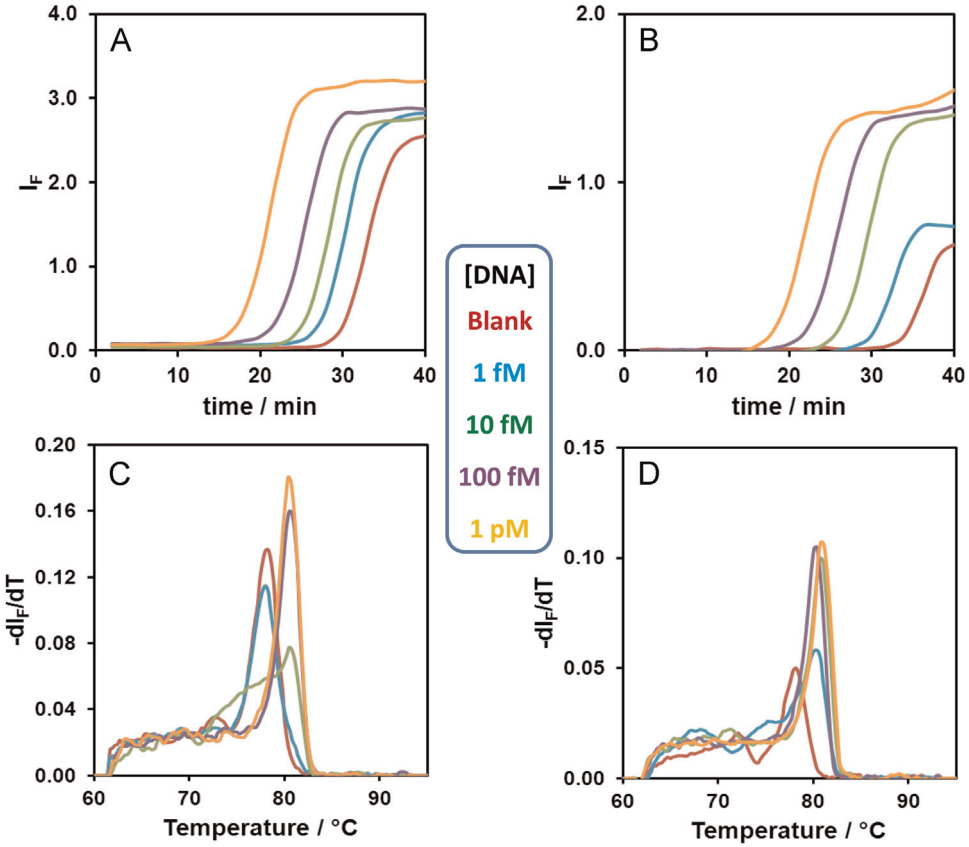

Fig. 1. Real-time amplification curves for 200 nM (A) and 75 nM (B) of primers. First derivative plots of the melting curves obtained for the end products are represented in (C) and (D), respectively.

obtained (Fig. 1A and B). The threshold time (t_T) i.e. the reaction time required for fluorescent intensity exceeds a threshold set right above the background fluorescence intensity, is a function of the concentration of input target DNA. Amplification speed, which may be represented by the inverse of this time, increases as target concentration increases, and it is also higher at higher primer concentration. However, this does not necessarily provide lower detection limits, since template-free amplification also occurs after shorter reaction times for the higher amount of primers. Only melting curve analysis of the final products allows discriminating non-specific products vs. specific ones, which are observed in the corresponding first derivative plots as peaks with different melting temperature (Fig. 1C and D). The analysis of these curves reveals that for 75 nM primers 1 fM DNA gives rise to products different from blank, whereas amplification with 200 nM primers produces specific amplicons only from 10 fM of target.

We obtained a good linear correlation between the threshold time and the initial target copy number (log scale) for both amounts of primers. The linear least squares fittings are

200 nM primers: $t_T/\text{min} = (-3.9 \pm 0.3)\log_{10}(\text{DNA copy number}) + (48 \pm 2)$; $R^2 = 0.996$
75 nM primers: $t_T/\text{min} = (-4.2 \pm 0.1)\log_{10}(\text{DNA copy number}) + (52.2 \pm 0.4)$; $R^2 = 0.999$

This behavior suggests exponential reaction kinetics during the initial phase of the reaction ($N_t = N_0 E^t$, where N_t represents the number of copies after amplification, N_0 is the initial number of target DNA copies, and E is the amplification efficiency). From this model, amplification efficiencies very similar in both cases, namely 1.80 ± 0.07 for 200 nM primers and 1.73 ± 0.03 for 75 nM primers, are obtained. However, the detection limit is 10-fold higher for the highest primer concentration due to non-specific amplification caused by mispriming or primer–dimers. This background amplification can lead to false positive results (Mahalanabis et al., 2011), limiting the detectability of the assay unless a sequence specific detection can be performed.

3.2. Coupling HDA to electrochemical detection

It would be a significant advance to be able to use a hybridization-based electrochemical assay for its direct coupling to HDA amplification, without further purification, reducing background signal amplification, and thus improving the limit of detection. To this aim we selected an asymmetric HDA format by employing a limiting amount of one of the primers, the direct one. In this way, when the concentration of this primer is depleted, the reaction switches to linear amplification of biotinylated single-stranded products for which higher efficiency of hybridization is expected in the subsequent electrochemical detection. Besides, this asymmetric design will contribute to reduce the background amplification, maximizing the yield of specific products versus non-specific ones.

The amount of amplicon for an initial template concentration 1 pM was quantified as a function of primer ratio, using a molar ratio between reverse and forward primers in the range 5–100 with an amount of the reverse primer fixed in 75 nM. The yield of detectable amplicon was found to be particularly sensitive to the ratio of starting primers, with a decreased production at ratios higher than 15. Meanwhile background amplification asymptotically decreased as the limiting primer decreased, in agreement with a primer–dimer origin of non-specific amplification. Such behavior led to a maximum signal to blank ratio (S/B) for a direct primer concentration 5 nM, 15 times less than the concentration of

the biotinylated reverse primer (Fig. S2).

A key feature to achieve further suppression of the background is to perform the post-amplification molecular recognition step, namely the hybridization reaction, under conditions that allow discrimination among sequences with different binding strengths. Stringency of the hybridization is usually controlled by salt concentration, so we tested two different ionic strengths for this step: 0.1 M and 1 M sodium chloride in the hybridization buffer (5 mM Tris–HCl, pH 7.40). We observed that the lower the salt concentration the lower the background signal, while the signal for the sample is not altered (Fig. S3). This means that S/B, which serves as indicator of specificity, increases when salt concentration decreases, obtaining an S/B value of 100 for 1 fM initial target concentration in the presence of 0.1 M NaCl in the hybridization solution; this ionic strength was selected for further assays. Under these conditions we use the Mfold Web Server (Zuker, 2003) for calculating the Gibbs energy for hybridization between target and signaling probe at 25 °C which is −24.3 kcal/mol. Another parameter that affects the kinetics of hybridization is the concentration of the signaling probe. We observed that for achieving maximum sensitivity its concentration should be at least equal to the concentration of the excess primer, 75 nM (Fig. S4).

Under these conditions, we verified the use of the complete assay as a quantitative indicator of *M. tuberculosis* by performing 90 min amplification reactions with different initial concentrations of the synthetic target. We found that our assay recognizes the target at concentrations as low as 1 aM and saturates around 1 fM (Fig. 2). There is a strong correlation between the current we measured in the assay and the initial target concentration at very low concentrations, with a linear relation up to 100 aM ($i/\mu A = (0.065 \pm 0.004)$ [MTB]/aM + (0.02 ± 0.2); $R^2 = 0.992$; inset of Fig. 2). The corresponding chronoamperograms are presented in Fig. S5. This linear relationship suggests linear amplification during the formation of ssDNA at this concentration range. The complete assay displays high reproducibility, with a RSD of 2.3% at 100 aM concentration level. The limit of detection, estimated as $3s_b/m$ (where s_b is the standard deviation of the blank and m is the slope of the calibration graph), is 0.5 aM which corresponds to only 15 target sequences, and approximately 1 bacteria cell in 50 μL of sample when we take into account the average number of repetitions per genome of the insertion fragment selected as target (Cole et al., 1998). This is approximately 3.2×10^3 times lower than the previously reported real-time homogeneous electrochemical detection of HDA products (Kivlehan et al., 2011), 6×10^9 times better than the heterogeneous one (Torres-Chavolla and Alocilja, 2011) and three orders of magnitude more sensitive than the same real-time fluorometric assay.

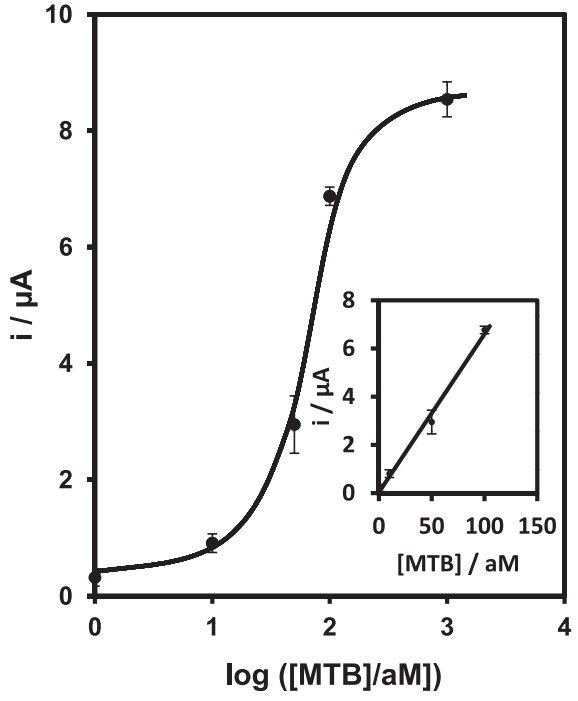

Fig. 2. Dependence of the measured current and the initial target concentration in the quantification of MTB with aHDA and electrochemical detection. Inset represents the response in the linear range.

The characteristics of the complete assay were compared with the analytical performance of the genomagnetic assay without amplification, using synthetic DNA analogs of the amplification products. In this case, a linear calibration plot is obtained in the range 5–200 pM ($i/\mu A = (0.0176 \pm 0.0004)$ [MTB]/pM + 0.02 ± 0.03; $R^2 = 0.998$), with a limit of detection of 0.5 pM, 10^6 fold higher than the limit of detection of the complete assay, that is, with HDA amplification. We verified that when dsDNA is used as target in the genomagnetic assay, signals not significantly different from blank are obtained. To achieve a favorably competition between the signaling probe and the complementary strand is necessary to heat the solution containing dsDNA and the signaling probe at 98 °C for 5 min, followed by a rapid cooling on ice before its entrapment on the magnetic beads. Under these conditions a linear calibration graph with a sensitivity of 22 nA pM^{-1} similar to that reported for ssDNA is obtained, but the isothermal conditions are not maintained throughout the test.

The selective detection of ssDNA in the presence of dsDNA under the isothermal conditions enabled us to calculate the number of copies of ssDNA obtained after asymmetric amplification as a function of the initial ones. In this way, we estimate that the linear amplification of the 84 bases long sequence specific of MBT is about 3×10^6 folds in 90 min.

A reduction in the amplification time from 90 min to 60 min results in signals not significantly different from negative controls even for an initial target concentration of 1 fM. On the contrary, when we used a symmetric amplification format (sHDA) in the presence of 75 nM each primer, coupled to homogeneous hybridization with the signaling probe after heating the mixture to 98 °C prior capturing onto the magnetic beads, 10 aM target concentration gives a signal 2.7 times the negative control after only 30 min amplification reaction (Fig. 3). Thus, as expected, kinetics of the symmetric amplification is faster than asymmetric one (aHDA). However, symmetric amplification for 60 min leads to an increase in the background amplification, more than 100 times larger than for 30 min, meaning that selecting the amplification time is crucial for both amplifying the correct product and limiting the non-specific amplification. In addition, comparing the analytical performance of both assays i.e. 90 min aHDA versus 30 min sHDA, we observed much smaller signals for the symmetric one and a limit of detection one order of magnitude lower. With sHDA we obtained double-stranded amplified fragments, and consequently during hybridization the complementary strand will compete with the signaling probe, giving rise to lower hybridization efficiency. Therefore, the detection signal and the sensitivity of detection are lower than when preferably ssDNA targets are obtained (aHDA), as it was previously described for PCR (Poddar, 2000).

To evaluate the selectivity of our design we tested DNA extracts from cultures of other respiratory pathogens i.e. *Legionella pneumophila*, *Pseudomonas* and *Staphylococcus* at a 3×10^8 cfu/mL level. No significant differences with respect to the negative control were observed, clearly supporting the specificity of the assay (Table S2 and Fig. S6).

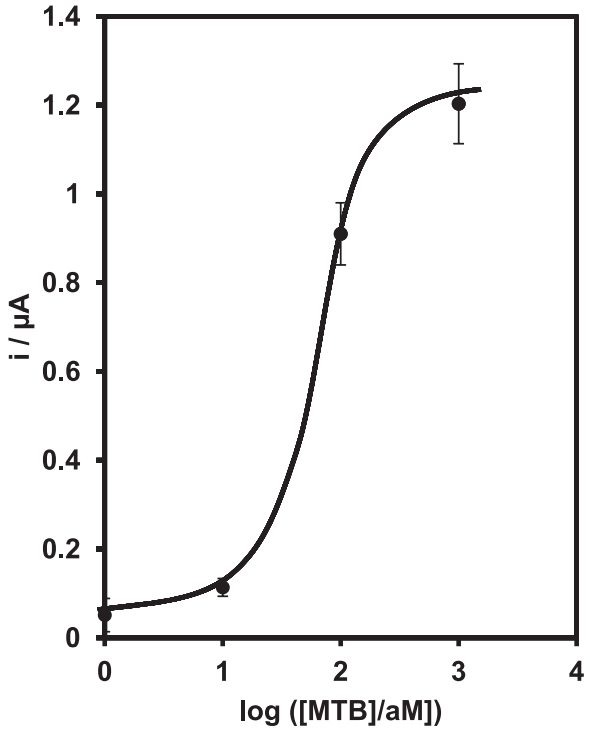

Fig. 3. Dependence of the measured current and the initial target concentration in the quantification of MTB with sHDA and electrochemical detection. Amplification time: 30 min.

3.3. Detection of bacterial genomic DNA in clinical samples

To demonstrate the practical utility of the assay, we evaluated different clinical samples provided by the Regional Reference Unit of Mycobacteria in Asturias. These include three sputum, one pleural fluid and two urine samples (Table 1). Of these, one sputum sample was negative by microscopic examination of smears stained with the Ziehl–Neelsen stain, the remaining were smear-positive specimens. All the tested samples were culture positive for MTB, which takes 3–8 weeks, and had different bacterial load as estimated by microscopic observation and RTi-PCR Xpert®MTB/RIFA, which is recognized as one of the most sensitive and with highest diagnostic accuracy among commercial PCR tests for tuberculosis detection (Steingart et al., 2013). For each sample three or more replicates were obtained using the aHDA-genomagnetic assay. To rule out potential false negatives arising from

Table 1
Comparison of the results obtained for MBT clinical specimens using the complete genoassay expressed as signal to negative control (*S*/*B*) and the standard methods.

Microscopic observation (No. AFB/field)	Culture	RTi-PCR[a]	HDA-genoassay (*S*/*B*)
Sputum			
No AFB observed	+	26 (Low)	1.2 ± 0.2
1-9 AFB/300 fields	+	21 (Medium)	8.5 ± 0.5
1-9 AFB/field	+	12 (High)	99 ± 3
Urine			
1-9 AFB/300 fields	+	23 (Medium)	4.4 ± 0.6
1-9 AFB/100 fields	+	21 (Medium)	25 ± 5
Pleural fluid			
1-9 AFB/10 fields	+	15 (High)	41 ± 9

[a] C_t value, the cycle of detection of products (qualitative estimation of the bacillary load).

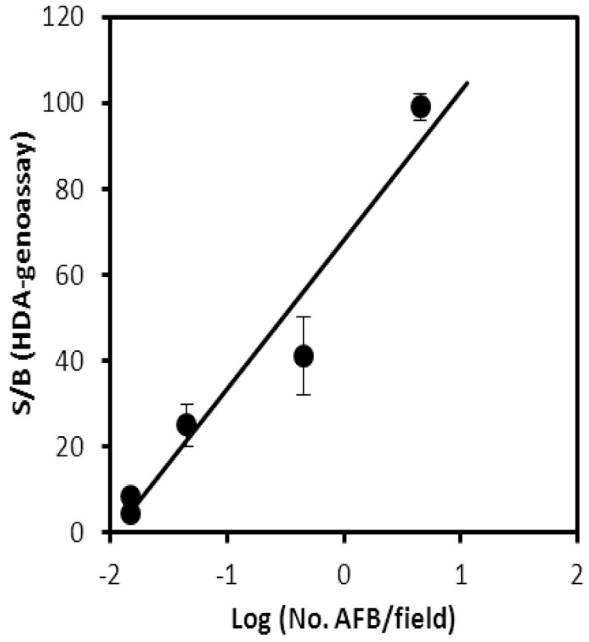

Fig. 4. Linear correlation between *S*/*B* ratio obtained in the HDA-genomagnetic assay and the bacillary load obtained by the smear test. $S/B = 35 \log(\text{No AFB/field}) + 68$; $R^2 = 0.945$.

inhibition of the amplification due to other matrix components, we always tested the same sample spiked with 1 fM synthetic target (3×10^4 copies) as internal control.

Our assay detects *M. tuberculosis* in the three matrices assayed, giving bacillary loads in agreement with those obtained by PCR and microscopic observation. In all cases, internal control to signal ratio (IC/*S*) was significantly higher than one, thus excluding false negatives caused by sample inhibition of amplification. In addition we observed that the higher the bacterial load in the sample the lower IC/*S* is (Fig. S7). Nevertheless, *S*/*B* ratio is the most suitable value for expressing in a more intuitive way the quantitative results. There is a strong correlation between this value and the number of AFB/field obtained in the microscopic observation (Fig. 4). The aHDA-genomagnetic assay was positive for five of six specimens that were culture positive for MTB. The negative sample was also negative by acid fast-smear. Our assay is thus capable of discriminating medium and high bacillary loads in respiratory and urine samples within approximately 4 h.

4. Conclusions

We have developed a method for the electrochemical quantification of very small quantities of pathogenic genomic DNA. By selecting an asymmetric format for HDA we straightforwardly address the unspecific amplification problems associated to most isothermal nucleic acid quantification strategies, achieving an amplification factor $> 10^6$ folds. Our platform is capable of detecting as few as 0.5 aM of synthetic target, which corresponds to 15 copies of MBT genome, under isothermal conditions in less than 4 h and it has been successfully applied to the detection of *M. tuberculosis* in sputum, pleural fluid and urine samples. The robustness, speed and sensitivity of this method suggests it could be applied for the rapid quantification of small amounts of other specific DNA sequences, not only of clinical relevance but also in the field of food and environmental analysis, taking full advantage of the plethora of information that the post-genomic era is offering. Additionally, it constitutes a step toward the development of portable and widely accessible nucleic acid tests.

Acknowledgments

Authors thank Dr. José Luis Martínez Fernández and other members of the Biotechnological and Biomedical trials Unit in the Scientific and Technical Services of the University of Oviedo for technical assistance in PCR and HDA amplification and sequencing. This work has been supported by Ministerio de Economía y Competitividad (Spain) Projects CTQ2008-02429 and CTQ2012-31157, and the European Regional Development Fund.

Appendix A. Supplementary material

Supplementary data associated with this article can be found in the online version at http://dx.doi.org/10.1016/j.bios.2014.12.029.

References

Andresen, D., von Nickisch-Rosenegk, M., Bier, F.K., 2009. Clin. Chim. Acta 403, 244–248.
Ao, W., Aldous, S., Woodruff, E., Hicke, B., Rea, L., Kreiswirth, B., Jenison, R., 2012. J. Clin. Microbiol. 50, 2433–2440.
Barbieri, D., Venturoli, S., Rösl, F., Rincon-Orozco, B., 2014. Diagn. Microbiol. Infect. Dis. 79, 178–182.
Cole, S.T., et al., 1998. Nature 393, 537–544.
Connolly, A.R., Trau, M., 2010. Angew. Chem. Int. Ed. 49, 2720–2723.
Corrigan, D.K., Schulze, H., Henihan, G., Hardie, A., Ciani, I., Giraud, G., Terry, J.G., Walton, A.J., Pethig, R., Ghazal, P., Crain, J., Campbell, C.J., Templeton, K.E., Mount, A.R., Bachmann, T.T., 2013. Analyst 138, 6997–7005.
Craw, P., Balachandran, W., 2012. Lab Chip 12, 2469–2486.
Hataoka, Y., Zhang, L., Mori, Y., Tomita, N., Notomi, T., Baba, Y., 2004. Anal. Chem. 76, 3689–3693.
Hill, H.D., Vega, R.A., Mirkin, C.A., 2007. Anal. Chem. 79, 9218–9223.
Hsieh, K., Patterson, A.S., Ferguson, B.S., Plaxco, K.W., Soh, H.T., 2012. Angew. Chem. Int. Ed. 51, 4896–4900.
Jordan, J.A., Ibe, C.O., Moore, M.S., Host, C., Simon, G.L., 2012. J. Clin. Virol. 54, 11–14.
Kivlehan, F., Mavré, F., Talini, L., Limoges, B., Marchal, D., 2011. Analyst 136, 3635–3642.
Li, J., Macdonald, J., 2015. Biosens. Biolectron. 64, 196–211.
Lucarelli, F., Marrazza, G., Mascini, M., 2005. Biosens. Bioelectron. 20, 2001–2009.
Mahalanabis, M., Do, J., AlMuayad, H., Zhang, J.Y., Klapperich, C.M., 2010. Biomed. Microdevices 12, 353–359.
Mahalanabis, M., Do, J., AlMuayad, H., Zhang, J.Y., Klapperich, C.M., 2011. Biomed. Microdevices 13, 599–602.
Martín-Fernández, B., Miranda-Ordieres, A.J., Lobo-Castañón, M.J., Frutos-Cabanillas, G., de-los-Santos-Álvarez, N., López-Ruíz, B., 2014. Biosens. Bioelectron. 60, 244–251.
Minunni, M., Tombelli, S., Fonti, J., Spiriti, M.M., Mascini, M., Bogani, P., Buiatti, M., 2005. J. Am. Chem. Soc. 127, 7966–7967.
Miranda-Castro, R., de-los-Santos-Álvarez, N., Lobo-Castañón, M.J., Miranda-Ordieres, A.J., Tuñón-Blanco, P., 2009. Biosens. Bioelectron. 24, 2390–2396.
Motré, A., Kong, R., Li, Y., 2011. J. Microbiol. Methods 84, 343–345.
Nam, J.M., Stoeva, S.I., Mirkin, C.A., 2004. J. Am. Chem. Soc. 126, 5932–5933.
Niemz, A., Ferguson, T.M., Boyle, D.S., 2011. Trends Biotechnol. 29 (5), 240–250.
Notomi, T., Okayama, H., Masubuchi, H., Yonekawa, T., Watanabe, K., Amino, N., Hase, T., 2000. Nucleic Acids Res. 28, e63.
Pedrero, M., Campuzano, S., Pingarrón, J.M., 2011. Anal. Methods 3, 780–789.
Poddar, S.K., 2000. Mol. Cell. Probes 14, 25–32.
Ramalingam, N., San, T.C., Kai, T.J., Mak, M.Y.M., Gong, H.Q., 2009. Microfluid Nanofluid 7, 325–336.
Sassolas, A., Leca-Bouvier, B.D., Blum, L.J., 2008. Chem. Rev. 108, 109–139.
Shen, F., Davydova, E.K., Du, W., Kreutz, J.E., Piepenburg, O., Ismagilov, R.F., 2011. Anal. Chem. 83, 3533–3540.
Shi, C., Liu, Q., Ma, C., Zhong, W., 2014. Anal. Chem. 86, 336–339.
Steingart, K.R., Sohn, H., Schiller, I., Kloda, L.A., Boehme, C.C., Pai, M., Dendukuri, N., 2013. Cochrane Database of Systematic Reviews Issue 1. Art. No.: CD009593. http://dx.doi.org/10.1002/14651858.CD009593.pub2.
Tan, E., Wong, J., Nguyen, D., Zhang, Y., Erwin, B., Van Ness, L.K., Baker, S.M., Galas, D.J., Niemz, A., 2005. Anal. Chem. 77, 7984–7992.
Tanaka, Y., Xi, H., Sato, K., Mawatari, K., Renberg, B., Nilsson, M., Kitamori, T., 2011. Anal. Chem. 83, 3352–3357.
Tong, Y., McCarthy, K., Kong, H., Lemieux, B., 2012. J. Mol. Diagn. 14, 569–576.
Torres-Chavolla, E., Alocilja, E.C., 2011. Biosens. Bioelectron. 26, 4614–4618.
Vincent, M., Xu, Y., Kong, H., 2004. EMBO Rep. 5, 795–800.
Zhao, W., Ali, M.M., Brook, M.A., Li, Y., 2008. Angew. Chem. Int. Ed. 47, 6330–6337.
Zuker, M., 2003. Nucleic Acids Res. 31, 3406–3415.